Feedback-enhanced sensitivity in optomechanics: Surpassing the parametric instability barrier

Glen I. Harris,[1] Ulrik L. Andersen,[2] Joachim Knittel,[1] and Warwick P. Bowen[1]

[1]*Centre for Engineered Quantum Systems, University of Queensland, St. Lucia, Queensland 4072, Australia*
[2]*Department of Physics, Technical University of Denmark, Building 309, 2800 Lyngby, Denmark*

The intracavity power, and hence sensitivity, of optomechanical sensors is commonly limited by parametric instability. Here we characterize the degradation of sensitivity induced by parametric instability in a micron-scale cavity optomechanical system. Feedback via optomechanical transduction and electrical gradient force actuation is applied to suppress the parametric instability. As a result a 5.4-fold increase in mechanical motion transduction sensitivity is achieved to a final value of 1.9×10^{-18} mHz$^{-1/2}$.

PACS number(s): 42.50.Pq, 07.10.Cm

Optical techniques are capable of ultraprecise measurements of parameters such as phase, position, and refractive index. The sensitivity is typically limited by optical shot noise, which can be reduced by increasing optical power. Using coherent states of light the ultimate sensitivity is fundamentally set by the standard quantum limit (SQL) [1,2]. However, well before the SQL is reached, radiation pressure may become sufficiently strong to severely alter the dynamics of the intrinsic mechanical motion of the sensor. This regime, called parametric instability, is characterized by violent mechanical oscillations and was first theoretically investigated by Braginsky [3] in the context of large-scale interferometers for gravitational wave detection, followed by experimental observation in electrical readouts of resonant bar systems [4] and later in optical microcavities [5]. The physical process, described graphically in Fig. 1, is a result of radiation pressure from asymmetric Stokes and anti-Stokes sidebands generated from the mechanical motion of the cavity. If this process, known as dynamical backaction heating [6], amplifies the motion at a rate faster than the mechanical decay rate then parametric instability occurs. Due to a combination of large mechanical oscillations and necessary saturation of amplification, the noise floor of the optomechanical sensor increases, rendering it ineffective at transducing small signals. Consequently, parametric instability is predicted to be a problem in the context of ultraprecise optical sensors such as gravity wave interferometers [3].

Parallel to the development of gravitational wave detectors, there has been a recent push towards real-time readout and control of mesoscopic mechanical oscillators in the quantum regime [7–9], facilitating new quantum information technologies [10], and experimental tests of quantum nonlinear mechanics [11–13] and even potentially quantum gravity [14]. However, parametric instability limits the strength of both entangled and squeezed states which may be produced via the optomechanical interaction [15], and—even when employing strategies such as backaction evasion (BAE)—the ability to transduce the mechanical motion at the quantum level [16].

Radiation-pressure-mediated optomechanical interactions are also of increasing importance to photonic circuits and sensors, where many applications are facilitated by miniaturized integrated architectures [17,18]. Miniaturization is often accompanied by high mechanical compliance. This has the adverse consequence of increasing exposure to parametric instability but provides the possibility of introducing new functionality via mechanical elements such as optomechanical switches [19] and memories [20], and ultraprecise gyroscopes, magnetometers [21], and mass and force sensors [22]. Even hybrid optomechanical circuits have been proposed, where fully integrated phononic and photonic circuits are interfaced via the optomechanical interaction [23], with phononic elements used for memories, filters, and processing elements and photonic elements used for communication. Parametric instability can severely adversely affect the performance of such integrated optomechanical devices.

The growing role of complex optomechanical systems in both fundamental science and applications means that techniques capable of individually addressing and suppressing instabilities in optomechanical elements are of crucial importance. In this Rapid Communication, we propose and experimentally demonstrate such a technique based on optoelectromechanical feedback control, characterizing the parametric-instability-induced degradation in, and feedback-induced revival of, mechanical transduction sensitivity in a cavity optomechanical transducer. Our cavity optoelectromechanical system (COEMS), seen in Fig. 1, consists of a silica microtoroid integrating high Q mechanical and optical modes with strong electrical actuation [24]. Parametric instability of a 14-MHz mechanical mode is found to occur at optical powers of 60 μW, resulting in a drastic loss of broadband sensitivity for higher power levels and a maximum optomechanical sensitivity still a factor of 300 higher than the SQL. Stabilization of the parametric instability is achieved via a viscous damping force applied to the unstable mechanical mode using electric feedback. Narrowband filtering ensures that the feedback force is applied only at frequencies in close proximity to the unstable mode, allowing broadband sensitivities at the level of 1.9×10^{-18} mHz$^{-1/2}$ limited by available optical power.

The dynamical interaction between light and mechanical motion including radiation pressure F_{rad}, feedback F_{fb}, and thermal forces F_{T} can be described through the equations of motion [6]

$$m\left[\ddot{x} + \Gamma_0\dot{x} + \omega_m^2 x\right] = F_{\mathrm{rad}} + F_{\mathrm{T}} + F_{\mathrm{fb}}, \qquad (1)$$

$$\dot{a} = -[\gamma - i(\Delta_0 + gx)]a + \sqrt{2\gamma_{\mathrm{in}}}a_{\mathrm{in}}. \qquad (2)$$
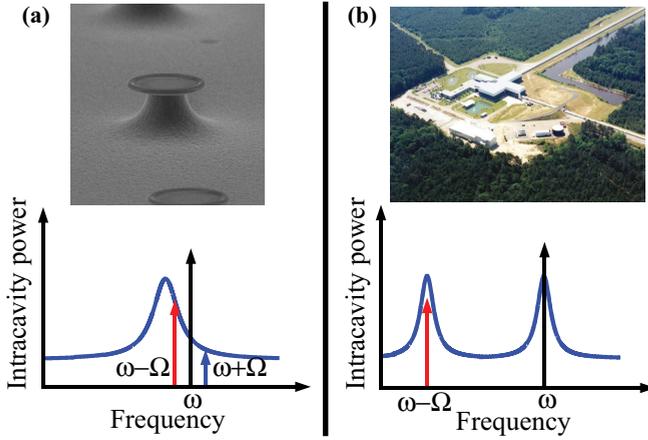
FIG. 1. (Color online) Ultrasensitive optomechanical systems exhibit parametric instability through cavity enhancement of the Stokes sideband produced by their mechanical motion. (a) In detuned micron-scale optomechanical systems Stokes and anti-Stokes sidebands spectrally overlap with the same optical mode. (b) In large-scale interferometers Stokes sidebands must overlap with an adjacent optical mode. Image of LIGO Livingston Laboratory courtesy of Skyview Technologies.

The first equation describes the motion of the mechanical oscillator where m, Γ_0, and ω_m are its effective mass, damping rate, and resonance frequency, respectively; $F_{\rm rad} = \hbar g |a(t)|^2$, and $F_{\rm T} = \sqrt{\Gamma_0 k_B T m} \xi(t)$, where $\xi(t)$ is a unit white-noise Wiener process. The second equation describes the intracavity optical field where Δ_0 is the optical detuning, $|a|^2$ is the intracavity photon number, and $|a_{\rm in}|^2$ is the input photon flux, coupled into the cavity at rate $\gamma_{\rm in}$. The total optical decay rate is $\gamma = \gamma_{\rm in} + \gamma_0$, where γ_0 is the intrinsic decay rate. The equations are coupled via the optomechanical coupling parameter, g, which gives rise to both static and dynamic effects such as radiation pressure bistability [25], the optical spring effect [26], and dynamical backaction cooling and amplification [27–30]. Due to the nonlinear nature of the equations of motion, linearization is required to reach an analytic solution where a separation of each variable into its mean value and fluctuations is performed; $a = \bar{a} + \delta a$ and $x = \bar{x} + \delta x$. Taking the linearized equations into the frequency domain yields

$$\delta a(\omega) = \frac{\sqrt{2\gamma_{\rm in}}\,\delta\tilde{a}_{\rm in} + ig\bar{a}\delta x(\omega)}{\gamma - i(\Delta - \omega)}, \qquad (3)$$

$$\chi_0^{-1}\delta x(\omega) = \hbar g[\bar{a}\delta a^\dagger(-\omega) + \bar{a}^*\delta a(\omega)] + F_{\rm T}(\omega) + F_{\rm fb}(\omega), \qquad (4)$$

where $\chi_0 = m^{-1}[\omega_m^2 - \omega^2 + i\Gamma_0\omega]^{-1}$ is the mechanical susceptibility and $\Delta = \Delta_0 + g\bar{x}$ is the static detuning of the cavity in the presence of radiation pressure. As seen in Eq. (3) the mechanical fluctuations are imprinted onto the field δa, which, in turn, is outcoupled with $a_{\rm out} = a_{\rm in} - \sqrt{2\gamma_{\rm in}}a$ and detected on a photodiode, giving a photocurrent $i = a_{\rm out}^\dagger a_{\rm out}$. After some work the resulting photocurrent fluctuation, $\delta i(\omega) = \bar{a}_{\rm out}^*\delta a_{\rm out} + \bar{a}_{\rm out}\delta a_{\rm out}^\dagger$, is found to be

$$\delta i = \delta x \left(\frac{2ig|\bar{a}|^2\Delta\,[\omega - i2\gamma_0]}{\gamma^2 + \Delta^2 - \omega^2 + i2\gamma\omega} \right) + \delta i_a, \qquad (5)$$

where δi_a contains all noise terms associated with the input field. This signal is then applied back onto the oscillator via the feedback force $F_{\rm fb}(\omega) = G\delta i$, where G is a complex feedback gain. Substituting this feedback force and the optical fluctuations, given by Eq. (3), into Eq. (4), an analytic form can be obtained for the modification of mechanical motion due to radiation pressure and feedback forces combined. The terms contributing to δx modify the mechanical susceptibility, χ, such that

$$\chi^{-1} = \chi_0^{-1} + \frac{2g|\bar{a}|^2\Delta\,[\hbar g + G(i\omega - 2\gamma_0)]}{\gamma^2 + \Delta^2 - \omega^2 + i2\gamma\omega}. \qquad (6)$$

If no feedback is applied, corresponding to $G = 0$, the mechanical susceptibility is modified purely by radiation pressure [29]. As is well known, the phase of the modulating radiation pressure depends on the sign of the detuning Δ, resulting in either mechanical linewidth narrowing or broadening. Parametric instability occurs when the modified mechanical linewidth is negative, with correspondingly exponential amplification of the mechanical oscillations. This amplification process eventually saturates to give a steady-state linewidth close to zero but positive. Similar to mode competition in a laser, this limits the parametric instability to one mechanical mode. Due to the large shifts of the optical resonance from amplified mechanical motion, the average intracavity power, and hence radiation pressure, decreases, resulting in saturation of the mechanical amplification. Since the mechanism for transduction is equivalent to actuation, the nonlinear saturation comes together with nonlinear transduction. This nonlinearity acts to mix different frequency components in the spectrum, resulting in broadband noise and hence severely degrading the transduction sensitivity. From Eq. (6) it can be seen that this degradation can be canceled and the original mechanical susceptibility recovered if the gain is chosen to be

$$G_{\rm crit} = \frac{\hbar g}{2\gamma_0 - i\omega}, \qquad (7)$$

such that all modifications to the mechanical susceptibility from radiation pressure are canceled by the electrical feedback. This simple expression is completely insensitive to fluctuations in the detuning Δ, the coupling rate $\gamma_{\rm in}$, and the input power $|a_{\rm in}|^2$, making the feedback system very robust against external noise sources. This robustness necessarily translates to simplicity of implementation, which is all important for optomechanical systems pushing towards the SQL. Many techniques have been proposed for the stabilization of parametric instabilities such as the addition of acoustic dampers, thermal control, and active feedback from a transduction signal using optical, electrical, or mechanical actuation [31], but feedback stabilization has to date been demonstrated only in large-scale low-frequency systems [32], where the parametric instability typically occurs due to the presence of many optical modes [Fig. 1(b)] rather than in one optical mode as is the case here [Fig. 1(a)], and with no characterisation of the degradation in sensitivity due to parametric instability or the enhancement achieved via active feedback.

Our experimental setup is shown in Fig. 2(a). A tunable diode laser at 780 nm was evanescently coupled into a microtoroidal whispering gallery mode using a tapered optical fiber. The microtoroid had major and minor diameters of
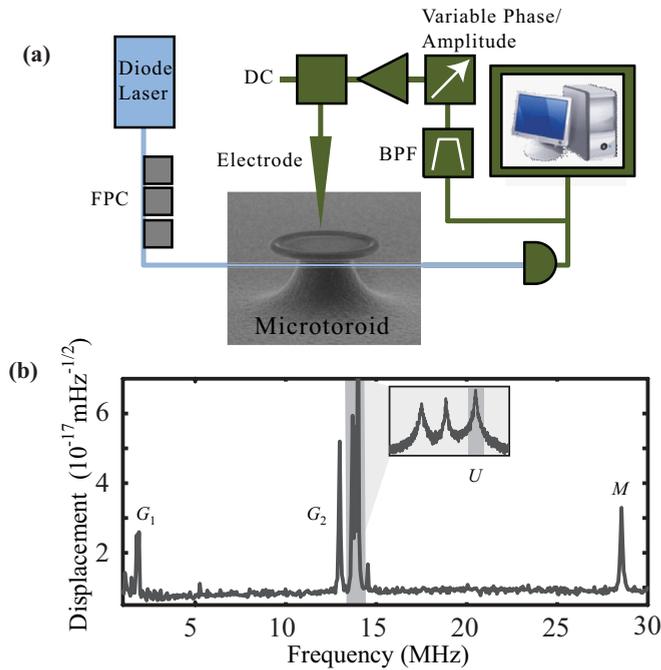
FIG. 2. (Color online) (a) Experimental schematic. Blue (light grey) indicates the optical components allowing transduction and parametric instability; green (dark gray) indicates the electrical components used in the feedback stabilization. FPC, fiber polarization controller; BPF, bandpass filter. (b) Observed mechanical spectra below parametric instability threshold.

60 μm and 6 μm respectively with a 26-μm undercut. The toroid-taper separation was controlled by a piezo stage to allow critical coupling into the optical cavity. The laser was thermo-optically locked [33,34] to the full-width half maximum (FWHM) of the optical mode, which had an intrinsic quality factor of $Q \approx 10^7$. This optical detuning allowed simultaneous radiation-pressure-induced mechanical amplification and transduction of the mechanical motion. The absolute mechanical displacement amplitude was calibrated via the optical response to a known reference phase modulation [35]. The mechanical motion, which modulates the optical resonance frequency, was detected via fluctuations in the transmitted power incident on an InGaAs photodiode. Fourier analysis of the photocurrent reveals a mechanical power spectra with peaks corresponding to mechanical resonances. A typical spectra containing many mechanical modes can be seen in Fig. 2(b) at optical powers below the threshold for parametric instability. At higher optical powers the unstable mode at 14 MHz, labeled U, experiences parametric instability. Here we focus on the effect of this process, with and without feedback stabilization, on the measurement of a mode at 28.6 MHz, labeled M. This mode was characterized experimentally to have an effective mass and linewidth of 0.3 μg and 90 kHz respectively, resulting in a standard quantum limit of $S_{\mathrm{SQL}}^{1/2} = \sqrt{\frac{\hbar}{2m_{\mathrm{eff}}\Omega_0\Gamma}} = 8 \times 10^{-21}$ mHz$^{-1/2}$.

Figure 3(a) shows that at low power the measured mode is easily resolved with the sensitivity improving with increasing optical power, as expected from photon shot noise statistics as a function of power. However, as the input power is increased above 60 μW the unstable mode experiences parametric
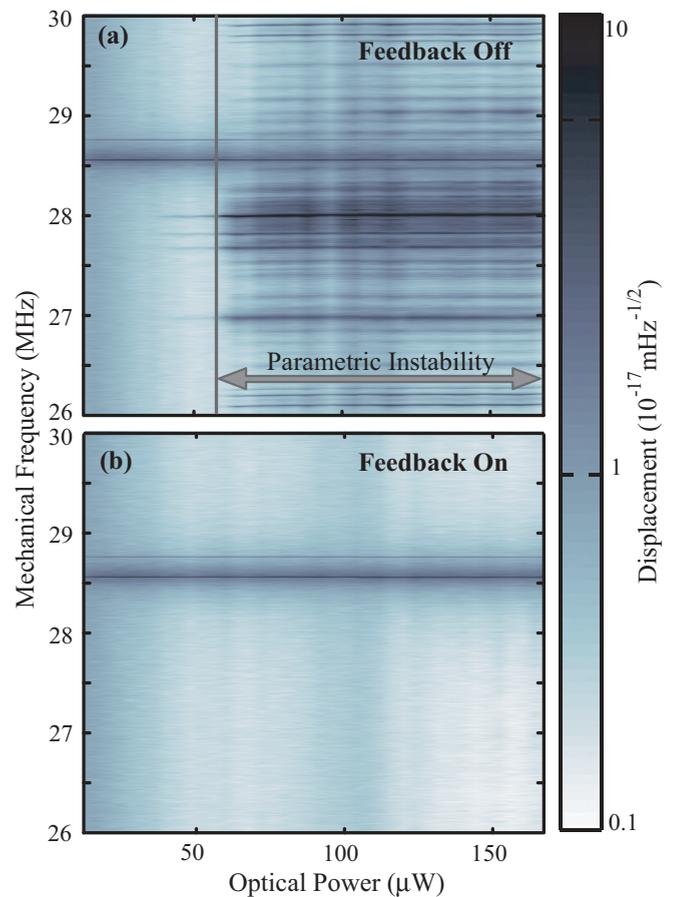

FIG. 3. (Color online) Mechanical power spectra show the mechanical spectra (b) with and (a) without feedback stabilization of the regenerative 14-MHz mode.

instability, generating harmonics on the transduction signal at 28, 42, and 56 MHz due to the nonlinear process involved in saturation. This is evident by the emergence of a dark narrow band, among broadband noise, at 28 MHz. The noise spectra at a fixed power of 136 μW is shown in Fig. 4(a) (dark line) and reveals the narrowed harmonic at 28 MHz, and beat frequencies from mixing with the groups of mechanical modes, labeled G_1 and G_2 in Fig. 2(b). The three peaks in the region labeled $U + G_2$ arise from sum frequency generation between the group G_2 and the unstable mode U, while the peaks in the regions $2U \pm G_1$ arise from sum and difference frequency generation, respectively, between group G_1 and the second harmonic of the unstable mode $2U$. In addition to these harmonics and beats, low-frequency laser phase noise, seen in the inset to Fig. 4(a), is also mixed up via sum and difference frequency generation with the second harmonic, causing broadband noise. This extra noise is clearly illustrated in Fig. 4(a) (dark trace), where mixed-up laser noise completely obscures the motion of the measured mode M (gray trace). The signal to noise ratio (SNR) of the measured mode is shown as a function of power in Fig. 4(b) (black squares), with severe degradation apparent once the threshold is reached.

Feedback to suppress the parametric instability was implemented by electrically filtering and amplifying the photocurrent and applying it directly to a sharp electrode placed close
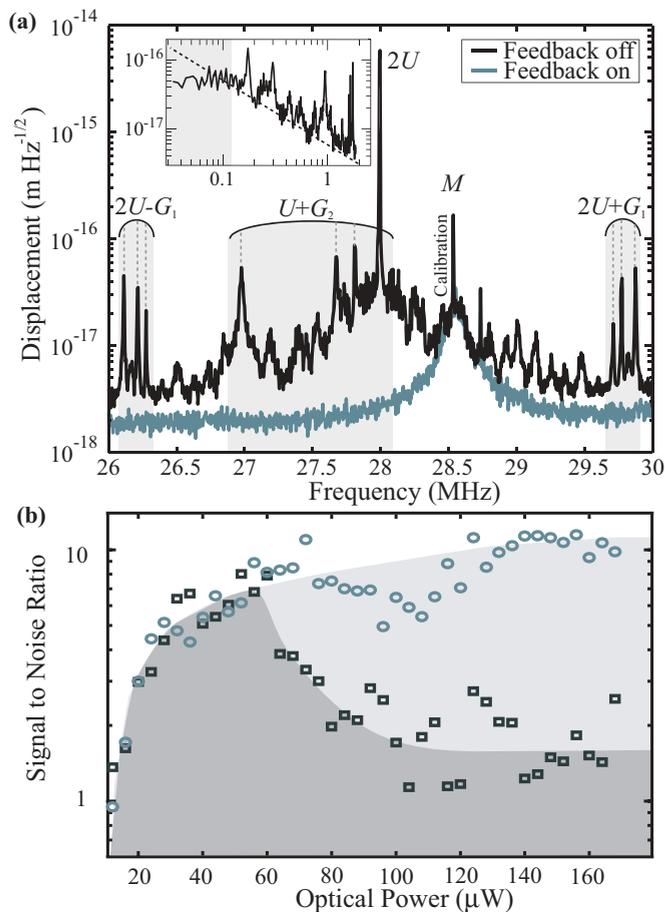
FIG. 4. (Color online) (a) Mechanical spectra observed with 136 μW of input power, well above the parametric instability threshold, with (gray) and without (black) feedback stabilization of the unstable 14-MHz mode. Inset: Single-sided noise spectrum about the second harmonic 2U (solid line) showing the measured scaling of laser frequency noise (dashed line) and the suppression of noise from thermal locking (shaded region). (b) Signal-to-noise ratio of the 28.6-MHz mechanical mode versus optical power with feedback (circles) and without feedback (squares).

to the microtoroid. This facilitated strong electrical actuation of the mechanical motion through electrical gradient forces [36]. Consecutive bandpass filters were used to isolate the unstable mechanical mode at 14 MHz, allowing maximum amplification of the feedback signal while eliminating the effect of feedback on the measured mode M. The feedback phase and gain were controlled inside the feedback loop by an

voltage variable phase shifter and attenuator respectively. With correct gain and phase as given in Eq. (7), the viscous damping force applied by feedback fully suppressed the parametric instability and eliminated the harmonics and associated noise from the unstable 14-MHz mode, as shown in Figs. 3(b) and 4(a) (light line). Consequently, the transduction sensitivity of the measured mode was found to improve with optical power, even above threshold, as shown in Fig. 4(b) (circles).

Parametric instability can in principle be circumvented without any feedback by operating in the zero- or red-detuned regime, rather than the blue-detuned regime used here. However, blue detuning is unavoidable in many circumstances. In room-temperature experiments with silica microtoroids such as those reported here, for example, the thermal response of silica causes intrinsic locking to the blue-detuned side of resonance [33]. To overcome this effect using electronic locking would require impractically high gain and bandwidth for the optical powers used in our experiments. Moreover, blue detuning is a requirement for many optomechanical protocols, such as optomechanical amplification [27,29,37], back-action evasion [16], entanglement, and mechanical squeezing [15]. It is also expected to be difficult to avoid in complex devices with many optomechanical elements such as gravity wave detectors and photonic-phononic circuits [3]. Our scheme provides a pathway to suppress instabilities in each of these circumstances. In complex optomechanical devices, for example, the feedback forces could be applied by electrodes integrated onto each optomechanical element, while the feedback signals could be obtained either directly from the optical output of the device with spectral filtering to select the appropriate unstable modes, or if there are degenerate unstable modes, from weak optical tapoffs integrated throughout the device.

This work represents an important step for stabilization in mesoscopic quantum optomechanical systems, particularly when involving BAE or optomechanical entanglement. Extending into applications, this technique could be used for stabilizing mechanical instabilities in miniaturized photonic-phononic circuits and mechanical sensors.

[1] C. M. Caves, K. S. Thorne, R. W. P. Drever, V. D. Sandberg, and M. Zimmermann, Rev. Mod. Phys. **52**, 341 (1980).

[2] J. D. Teufel, T. Donner, M. A. Castellanos-Beltran, J. W. Harlow, and K. W. Lehnert, Nat. Nano. **4**, 820 (2009).

[3] V. B. Braginsky, S. E. Strigin, and S. P. Vyatchanin, Phys. Lett. A **287**, 331 (2001).

[4] B. D. Cuthbertson, M. E. Tobar, E. N. Ivanov, and D. G. Blair, Rev. Sci. Instrum. **67**, 2435 (1996).

[5] H. Rokhsari, T. J. Kippenberg, T. Carmon, and K. J. Vahala, IEEE J. Sel. Top. Quantum **12**, 96 (2006).

[6] T. J. Kippenberg and K. J. Vahala, Opt. Express **15**, 17172 (2007).

[7] K. C. Schwab and M. L. Roukes, Phys. Today **58**, 36 (2005).

[8] A. D. O'Connell, M. Hofheinz, M. Ansmann, R. C. Bialczak, M. Lenander, E. Lucero, M. Neeley, D. Sank, H. Wang, M. Weides *et al.*, Nature (London) **464**, 697 (2010).

[9] J. D. Teufel, T. Donner, D. L. Li, J. W. Harlow, M. S. Allman, K. Cicak, A. J. Sirois, J. D. Whittaker, K. W. Lehnert, and R. W. Simmonds, Nature (London) **475**, 359 (2011).

[10] S. Mancini, D. Vitali, and P. Tombesi, Phys. Rev. Lett. **90**, 137901 (2003).

[11] M. J. Woolley, G. J. Milburn, and C. M. Caves, New J. Phys. **10**, 125018 (2008).

[12] R. Lifshitz, I. Katz, A. Retzker, and R. Straub, New J. Phys. **10**, 125023 (2008).

[13] D. Rugar and P. Grutter, Phys. Rev. Lett. **67**, 699 (1991).

[14] W. Marshall, C. Simon, R. Penrose, and D. Bouwmeester, Phys. Rev. Lett. **91**, 130401 (2003).

[15] D. Vitali, S. Gigan, A. Ferreira, H. R. Bohm, P. Tombesi, A. Guerreiro, V. Vedral, A. Zeilinger, and M. Aspelmeyer, Phys. Rev. Lett. **98**, 030405 (2007).

[16] K. C. Schwab, J. B. Hertzberg, T. Rocheleau, T. Ndukum, M. Savva, and A. A. Clerk, Nat. Phys. **6**, 213 (2010).

[17] V. R. Almeida, C. A. Barrios, R. R. Panepucci, and M. Lipson, Nature (London) **431**, 1081 (2004).

[18] R. X. Yan, D. Gargas, and P. D. Yang, Nat. Photon. **3**, 569 (2009).

[19] A. H. Safavi-Naeini, T. P. M. Alegre, J. Chan, M. Eichenfield, M. Winger, Q. Lin, J. T. Hill, D. E. Chang, and O. Painter, Nature (London) **472**, 69 (2011).

[20] M. Bagheri, M. Poot, M. Li, W. P. H. Pernice, and H. X. Tang, Nat. Nanotechnol. **6**, 726 (2011).

[21] S. Forstner, S. Prams, J. Knittel, E. D. van Ooijen, J. D. Swaim, G. I. Harris, A. Szorkovszky, W. P. Bowen, and H. Rubinsztein-Dunlop, Phys. Rev. Lett. **108**, 120801 (2012).

[22] M. Li, H. X. Tang, and M. L. Roukes, Nat. Nanotechnol. **2**, 114 (2007).

[23] H. S.-N. Amir and P. Oskar, New J. Phys. **13**, 013017 (2011).

[24] K. H. Lee, T. G. McRae, G. I. Harris, J. Knittel, and W. P. Bowen, Phys. Rev. Lett. **104**, 123604 (2010).

[25] A. Dorsel, J. D. McCullen, P. Meystre, E. Vignes, and H. Walther, Phys. Rev. Lett. **51**, 1550 (1983).

[26] B. S. Sheard, M. B. Gray, C. M. Mow-Lowry, D. E. McClelland, and S. E. Whitcomb, Phys. Rev. A **69**, 051801(R) (2004).

[27] O. Arcizet, P. F. Cohadon, T. Briant, M. Pinard, and A. Heidmann, Nature (London) **444**, 71 (2006).

[28] S. Gigan, H. R. Bohm, M. Paternostro, F. Blaser, G. Langer, J. B. Hertzberg, K. C. Schwab, D. Bauerle, M. Aspelmeyer, and A. Zeilinger, Nature (London) **444**, 67 (2006).

[29] T. J. Kippenberg, H. Rokhsari, T. Carmon, A. Scherer, and K. J. Vahala, Phys. Rev. Lett. **95**, 033901 (2005).

[30] P. F. Cohadon, A. Heidmann, and M. Pinard, Phys. Rev. Lett. **83**, 3174 (1999).

[31] L. Ju, D. G. Blair, C. Zhao, S. Gras, Z. Zhang, P. Barriga, H. Miao, Y. Fan, and L. Merrill, Class. Quantum Grav. **26**, 015002 (2009).

[32] T. Corbitt, D. Ottaway, E. Innerhofer, J. Pelc, and N. Mavalvala, Phys. Rev. A **74**, 021802 (2006).

[33] T. Carmon, L. Yang, and K. J. Vahala, Opt. Express **12**, 4742 (2004).

[34] T. G. McRae, K. H. Lee, M. McGovern, D. Gwyther, and W. P. Bowen, Opt. Express **17**, 21977 (2009).

[35] A. Schliesser, G. Anetsberger, R. Riviere, O. Arcizet, and T. J. Kippenberg, New J. Phys. **10**, 095015 (2008).

[36] T. G. McRae, K. H. Lee, G. I. Harris, J. Knittel, and W. P. Bowen, Phys. Rev. A **82**, 023825 (2010).

[37] T. G. McRae and W. Bowen, Appl. Phys. Lett. **100**, 201101 (2012).